diversity

MDPI

Article

Comparative Assessment of Shell Structural, Mechanical, and Elemental Properties in Adult Acorn Barnacles

Jazmine Shaw [1], Yeram Kang [1], Callie Triano [1], Corin J. Hoppe [1], Nick Aldred [2], Rebecca A. Metzler [3] and Gary H. Dickinson [1,*]

[1] Department of Biology, The College of New Jersey, Ewing, NJ 08628, USA
[2] School of Life Sciences, University of Essex, Colchester CO4 3SQ, UK
[3] Department of Physics and Astronomy, Colgate University, Hamilton, NY 13346, USA
* Correspondence: dickinga@tcnj.edu

Abstract: Balanomorph (acorn) barnacles are found throughout the world's coastal oceans, and their success is dependent on a hard, mineralized, outer shell. Although macro-scale morphology of barnacle shells has been studied extensively, relatively little is known about shell properties at the micron-scale and if such properties vary among species. We assessed shell structure, mechanics, and composition in seven species of balanomorph barnacles from five genera. Three species, *Amphibalanus amphitrite*, *Amphibalanus improvisus*, and *Austrominius modestus*, were laboratory-reared, enabling direct comparison of shell properties of barnacles grown under the same conditions for the same duration. Four other species, *Semibalanus balanoides*, *Amphibalanus eburneus*, *Chthamalus stellatus*, and *Tetraclita rubescens*, were field-collected. At the macro- and meso-scales, shell properties varied markedly among species, with differences in the number of shell plates, the presence of canals within the plates, mineralization of the base, and shell plate thickness. At the micron-scale, however, structure was remarkably similar among species. Plates of all species were constructed of irregular micron-scale crystallites, with a broad range of crystallite dimensions observed within the same shell. Similarly, micromechanical properties did not vary among species, regardless of testing orientation. Calcium carbonate was identified as calcite in all species assessed with no other mineral phases present, and calcium content did not vary among species. Hence, despite variation in the overall macro- and meso-scale morphology of barnacles, all appear to be built using the same, evolutionarily conserved, mineralization pathway.

Keywords: biomineralization; shell formation; crustacean; *Amphibalanus*; exoskeleton; calcite; mechanical properties; biofouling

Citation: Shaw, J.; Kang, Y.; Triano, C.; Hoppe, C.J.; Aldred, N.; Metzler, R.A.; Dickinson, G.H. Comparative Assessment of Shell Structural, Mechanical, and Elemental Properties in Adult Acorn Barnacles. *Diversity* **2024**, *16*, 482. https://doi.org/10.3390/d16080482

Academic Editor: Viatcheslav Ivanenko

Received: 3 July 2024
Revised: 29 July 2024
Accepted: 3 August 2024
Published: 8 August 2024

1. Introduction

Barnacles are found throughout the world's oceans, adhering tenaciously to both natural and anthropogenic substrates. As a type of biofouling organism—an organism that accumulates on human-made surfaces—they are well-known for attaching to docks, ships, and any other solid surfaces. Some, however, are also found attached to plants, vertebrates (e.g., whales and turtles), or other invertebrates (e.g., bivalves and crabs) within coastal and pelagic environments [1]. The presence of barnacles has a number of implications for the ecosystems in which they settle. For example, the shell of the barnacle may be a settlement substrate for other marine organisms (e.g., microbes, algae, other sessile invertebrates) and barnacles and their larvae are often prey for mobile predators and suspension feeders [2–4]. Additionally, they have a drastic economic impact on maritime industries by impacting hydrodynamics through their accumulation on ship hulls and other maritime structures [5,6].

Balanomorph (acorn) barnacles are typified by their conical, volcano-like shape [7]. They are sessile crustaceans surrounded by a hard, calcareous shell, which, in nearly all

species, is made up of a series of parietal plates (=wall plates) sitting directly atop a basal plate or membrane (Figure 1). Opercular plates articulate at the upper portion of the parietal plates, which can open to allow the feeding structures (cirri) to emerge [1,8]. This morphology is in contrast to pedunculate barnacles, in which the barnacle body, surrounded by mineralized plates, is suspended above the surface by a long, stalky peduncle that mediates adhesion to the substrate [9].

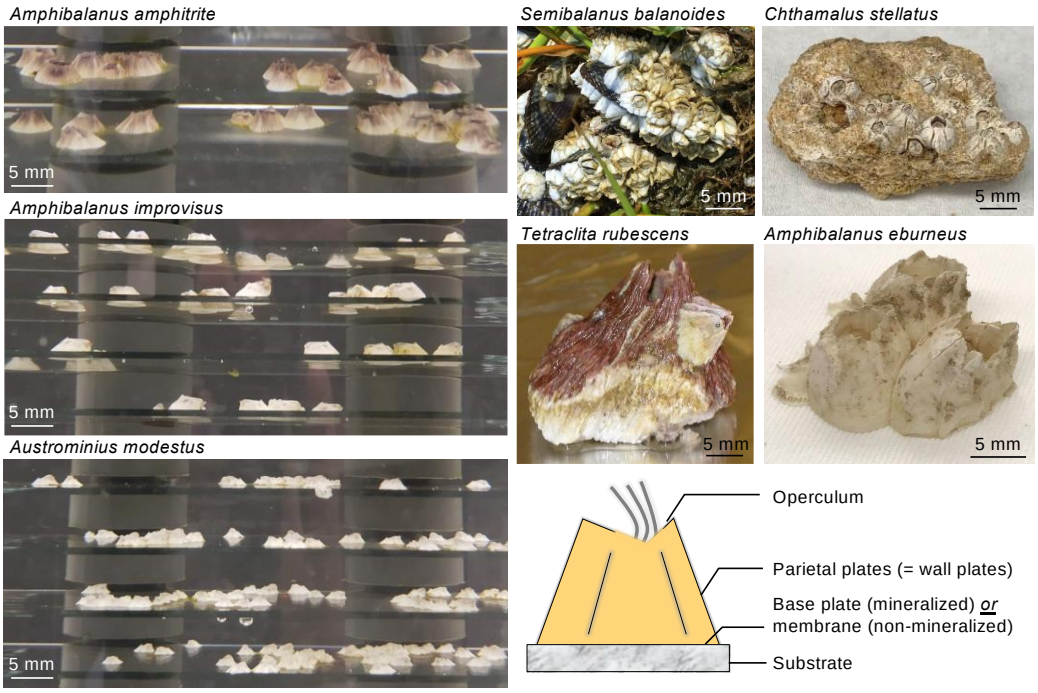

Figure 1. Photographs of the seven species of balanomorph barnacles assessed. *Am. amphitrite*, *Am. improvisus*, and *Au. modestus* were lab-reared, whereas *S. balanoides*, *C. stellatus*, *T. rubescens*, and *Am. eburneus* were field-collected. Bottom right shows relevant shell structures of a typical balanomorph barnacle.

Balanomorph barnacles are found in intertidal and subtidal zones as well as epibionts and parasites [1,2]. The shells of the barnacles serve as their sole means of defense against predation, protect the animals from wave action (including wave-born debris) and environmental stress (e.g., desiccation), and provide settlement cues for larvae [2,10–12].

The order Balanomorpha Pilsbury, 1916 comprises four monophyletic groups (superfamilies): Chthamaloidea, Elminoidea, Coronuloidea, and Balanoidea [8]. The number and assembly of parietal plates vary from one to eight among balanomorph barnacles, with six being the most common, and this characteristic has historically been used in phylogenetic assessments [8,13–16]. There is variation in macro- and meso-scale structures among different barnacle species, such as the number of parietal plates that make up the walls of the barnacle, whether there is a calcified or membranous base plate, the presence of canals running laterally through the plates, and the texture and coloration of the plates. For example, parietal plates of barnacles in the genus *Tetraclita* (Coronuloidea) contain a large number of canals and resemble a honeycomb, whereas barnacles in the genera *Austrominius* (Elminoidea) and *Chthamalus* (Chthamaloidea) completely lack canals within their parietal plates [8,17]. These meso-scale structural differences lead to variations in macro-scale mechanical properties [17–19]. What is consistent among the balanomorph barnacle species, however, is the fact that (with a few notable exceptions, e.g., *Xenobanalanus* spp., whale barnacles) they all share the irregular conical shape with a relatively flat bottom and shell plates composed of calcium carbonate [8,13,20].

Although macro- and meso-scale shell properties in Balanomorpha have been studied extensively, information on micron-scale structural and mechanical properties is limited.

Analysis of individual barnacles has shown that shell plates are composed primarily of highly irregular microstructures, exhibiting varying degrees of crystallographic orientation [20–24]. Shell-characterization efforts have typically focused on a single species, however, with few studies providing a direct comparison of multiple balanomorph species. Here, we characterized the shells of balanomorph barnacles from each major monophyletic group: four from Balanoidea (*Amphibalanus amphitrite*, *Amphibalanus improvisus*, *Amphibalanus eburneus*, and *Semibalanus balanoides*) and one each from Chthamaloidea (*Chthamalus stellatus*), Elminioidea (*Austrominius modestus)*, and Coronuloidea *(Tetraclita rubescens)*. We aimed to determine if structure at the meso- and micron- scale, micromechanical properties, and composition of barnacle shell plates vary among acorn barnacles of different genera. Given that biological materials are often anisotropic (vary in mechanical properties depending on testing orientation [25,26]) shells were tested in two orientations relative to the base plate. Together, these assessments provide insight on features that contribute to macro-scale shell strength among Balanomorpha.

2. Materials and Methods

2.1. Barnacle Collection, Larval Culture, and Analysis Overview

Barnacles were obtained from multiple sources for this study, leveraging larger projects on barnacle settlement, adhesion, and biomineralization. Photographs of the species assessed in this study can be found in Figure 1. Three species, *Amphibalanus amphitrite*, *Amphibalanus improvisus*, and *Austrominius modestus*, were lab-reared. Larval culture and settlement for these species was conducted at Newcastle University following well-established methods [27,28]. Larval culture was conducted at 28 °C, 25 psu for *A. improvisus* and *A. modestus*, 32 psu for *A. amphitrite*. Cyprids were settled on perfluoro-octyltrichlorosilane (PFOTS)-modified glass slides [29]. Once settled, juvenile barnacles of all three species were held at 28 °C, 28 psu. Juveniles were fed daily with *Tetraselmis suecica* for the first 6 weeks of growth, at which point, they transitioned to a diet of *Artermia* sp. At approximately 12 weeks post-settlement, barnacles were shipped live to The College of New Jersey for analysis.

Four additional barnacle species, *Semibalanus balanoides*, *Amphibalanus eburneus*, *Chthamalus stellatus*, and *Tetraclita rubescens*, were field-collected. *S. balanoides* was collected at the Rutgers Marine Field Station (39°50.94′ N, 74°32.41′ W) at low tide, adhered to Atlantic ribbed mussels (*Geukensia demissa*). Live *S. balanoides* were collected on 26 June 2019 and held for approximately 1 week in the lab in artificial seawater (Instant Ocean), 28–30 ppt, and 20–22 °C. *Amphibalanus eburneus* was collected at the same location as *S. balanoides*, on PFOTS-modified glass slides that had been submerged at ~1 m depth for 15 weeks (16 July–25 October 2019). *C. stellatus* were collected from Palmahim Beach, Israel (31°55.36′ N, 34°41.58′ E) in January 2014, and *T. rubescens* samples were collected from the Scripps Oceanographic Institute Pier (32°51.93′ N, 117°15.22′ W) in September 2010. Hereafter, barnacles in the genus *Amphibalanus* will be abbreviated with "*Am*" and *Austrominius* with "*Au*" to avoid potential confusion if a one-letter genus abbreviation is used.

Analyses included a combination of structural (polarized light microscopy and scanning electron microscopy), micromechanical, and compositional (polymorph of calcium carbonate and elemental content) testing. The full quantitative dataset (plate thickness, microhardness, and elemental composition) is provided in the supplement (Table S1). Since environmental conditions and growth duration were unknown for field-collected species, statistical analyses were only performed for data collected on lab-reared species (*Am. amphitrite*, *Am. improvisus*, and *Au. modestus*). Environmental conditions and the duration of growth was the same for all lab-reared individuals.

2.2. Sample Preparation

Adult barnacles were cleaned and dissected to enable embedding and polishing. Outer shell surfaces were cleaned of sediment and biofilm by gently wiping surfaces with 70% ethanol or microorganic soap (Allied High Tech Products). The operculum of the barnacle

was separated, and the barnacle body and mantle tissue were removed as described in Nardone et al. [30]. For barnacles grown on glass slides or mussel shells, barnacles remained adhered to the substrate to avoid disturbing the base-substrate interface. Substrates were trimmed to fit into sample mounting cups using a water-cooled diamond band saw (Gryphon C-40), and the remaining substrate and barnacle shells were cleaned and rinsed. All samples were dried at room temperature for at least 24 h before being embedded.

Barnacle shells were embedded in epoxy resin (Allied High Tech EpoxySet or Pace Technologies Ultrathin plus or Epoxicure) to enable grinding and polishing. Shells were oriented within sample mounting cups in one of two directions: (1) base plate or membrane parallel to the bottom of the embedding cup; (2) base or membrane perpendicular to the bottom of the embedding cup. Samples were ground and polished as described in Nardone et al. [30] until a cross-section midway through the barnacle shell had been reached. Final polishing was completed with either 0.04 µm colloidal silica suspension or 0.05-µm alumina slurry. For shells mounted with the base parallel to the bottom of the embedding cup, this procedure resulted in an oval-shaped cross-section (transverse plane); whereas for shells mounted with the base perpendicular to the bottom of the embedding cup, grinding/polishing resulted in a roughly U-shaped cross-section (sagittal plane) through the longest axis of the parietal plates and through the base (Figure 2A).

2.3. Structural Assessments

Embedded and polished samples, oriented in both directions described above, were imaged under polarized light using a reflected light microscope (Zeiss Axioscope.A1 with a Zeiss, AxioCam 105 color camera; analyzer set to 90° for all images). Imaging was conducted under a 2.5× or 5× objective, depending on the size of the sample, and panoramic images of the entire sample were constructed using imaging software (Zeiss Zen V. 2.3). Methods for quantifying shell plate thickness followed Nardone et al. [30]. For samples oriented perpendicular to the base, a 200 × 200 µm grid was placed on each image using imaging software and plate thickness was measured each time the grid crossed the shell sample. The total number of measurements per sample varied depending on the size of the shell and the presence of a mineralized base, but in all cases at least 40 replicate measurements were made within parietal plates and 20 within the base plate, when present. For samples oriented parallel to the base, a total of 30 replicate measurements were made, spaced roughly evenly among the parietal plates (five per plate for species with six parietal plates and seven to eight for species with four parietal plates).

Scanning electron microscopy (SEM) imaging was conducted on embedded and polished samples using a field emission SEM (Hitachi SU5000). Samples were imaged uncoated, at low vacuum (50 Pa), 15kV accelerating voltage, 8 mm working distance. Images were collected at 5000× magnification in at least four regions of the parietal plates and two regions of the base (in species with a calcified base plate), distributed along the length of visible plates. All images were taken within a solid portion of the plate, at least 250 µm away from edges, canals, or plate joints. Maximum width of crystallites, defined here as the longest continuous linear dimension of visible crystallite, was measured in a random subsample of 20 crystallites for the images shown in Figure 2. Automated selection of random points for analysis and crystallite measurements were conducted using ImageJ Version 1.54 g.

2.4. Micromechanical Testing

Microhardness was tested on embedded and polished shell samples using a microindentation hardness tester (Mitutoyo HM-200). Testing was conducted using a 10 g load, 15 sec dwell time. For samples embedded parallel to the base, a total of five indents were made in each parietal plate; indents were spaced roughly evenly along the length of the plate at least 250 µm away from edges or longitudinal canals. This resulted in a total of 30 indents for *Am. amphitrite*, *Am. improvisus*, *Am. eburneus*, *C. stellatus*, and *S. balanoides* (shell composed of six parietal plates) and 20 indents for *Au. modestus* and *T. rubescens*

(shell composed of four parietal plates). For samples embedded perpendicular to the base, five indents were made in each visible parietal plate (typically two parietal plates visible in this orientation), and 10 indents were made in the base plate for species with a calcified base. In each case, indents were placed roughly evenly along the length of the plate and at least 250 µm away from edges or canals.

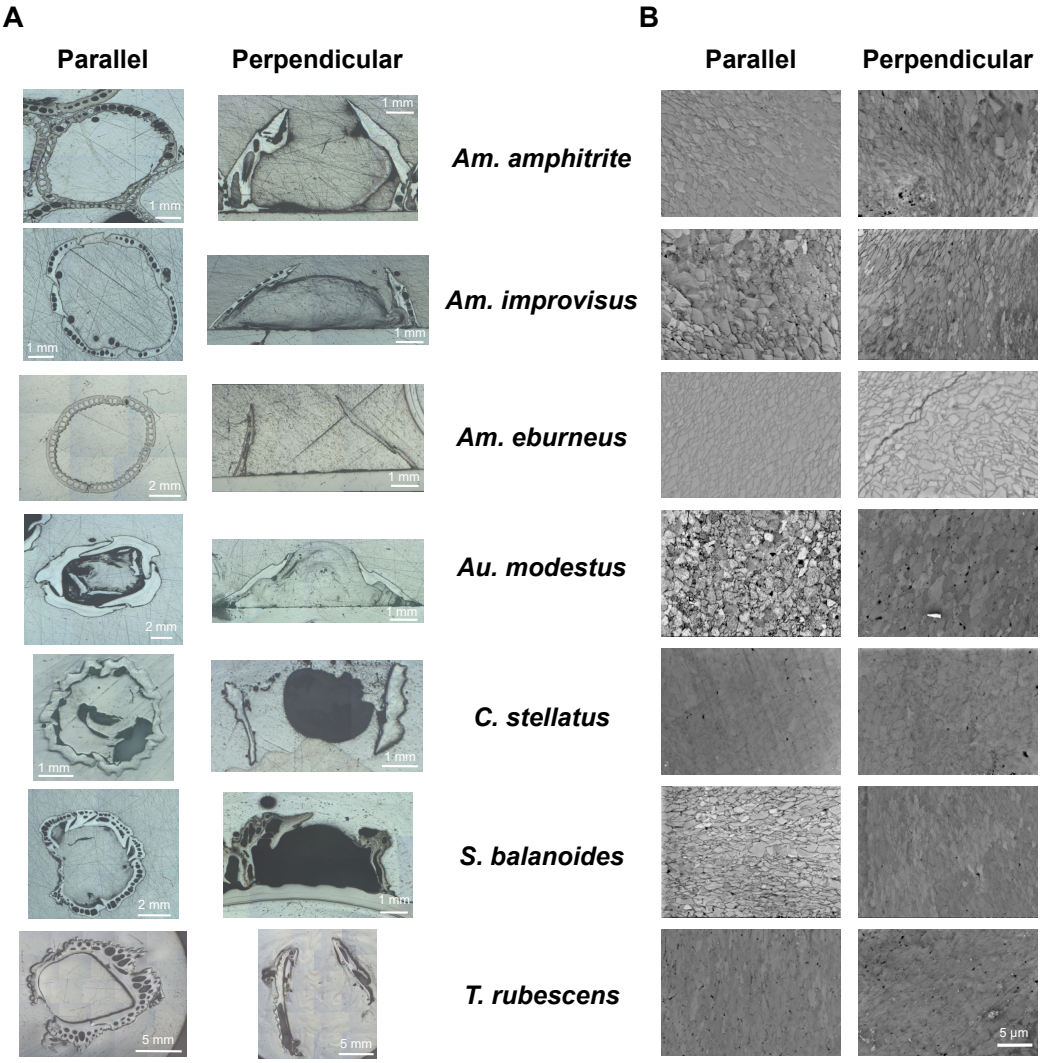

Figure 2. Representative polarized light (**A**) or scanning electron (**B**) microscopy images of seven species of barnacles. Shells were embedded and polished oriented either parallel to, or perpendicular to, the base. Polarized light microscopy illustrates calcium carbonate crystals of different c-axis orientations with different grey levels; variation in grey level, corresponding to differently oriented crystallites, was observed to varying extents in all species examined. Displayed SEM images were taken within parietal plates, in a central portion of the plate, away from any plate boundaries. For SEM images, the scale bar in the lower right applies to all images (5000× agnification in all cases), whereas the scale bars are marked individually for each light microscopy image.

2.5. Shell Composition

Fourier-transform infrared (FTIR) spectroscopy was used to assess the polymorph of calcium carbonate present in shell plates. Barnacle shells were collected, cleaned, and dissected as described previously, but shells were not embedded or polished. Rather, for each shell, parietal plates were removed from the base and crushed into a fine powder using a mortar and pestle. Powdered samples were placed on the ATR (attenuated total reflectance) crystal and compressed to a uniform force on a PerkinElmer Spectrum Two or Spectrum 100 spectrometer.

Spectra were collected at 4 wavenumber resolution, with 32 scans per sample, and were normalized and baseline corrected within the 600–2000 cm^{-1} region.

Elemental composition was determined using energy dispersive X-ray spectroscopy (EDS) during SEM imaging (AMTEK Materials Analysis Division, Octane Plus EDS detector). Spectra were acquired for full area scans at 5000× magnification in four different regions of the parietal plates and two regions of the base (in species with a calcified base plate). Imaging conditions resulted in a count rate of 8000–10,000 counts per second.

2.6. Statistical Analyses

Statistical analyses were conducted for shell plate thickness, microhardness, and calcium content using SPSS (V. 27, IBM Analytics). Replicate measurements within the same individual shell sample and shell region (base plate or parietal plates) were treated as technical replicates and were averaged to determine the mean value for each sample. Among technical replicates, outliers were identified as values greater than three times the interquartile range below or above the first or third quartile, respectively, and were removed from the dataset. For lab-reared species, the effect of species identity (*Am. amphitrite*, *Am. improvisus*, or *Au. modestus*) was assessed separately for thickness, microhardness, and calcium content using a one-way ANOVA, followed by Tukey HSD post hoc testing. Assumptions of normality and equal variance were assessed using Shapiro-Wilk and Levene tests, respectively, and data were log transformed, if necessary, to meet these assumptions. Data from the two orientations tested (parallel to, or perpendicular to, the base) were analyzed separately, since data were collected on different individuals for each orientation.

3. Results

3.1. Structure

Shells varied among species at the macro- (whole shell) and meso- (individual shell plate) scales (Figures 1 and 2A). Barnacles in the genus *Amphibalanus* were composed of six parietal plates and a mineralized base plate. *S. balanoides* and *C. stellatus* were also composed of six parietal plates but lacked a mineralized base (i.e., the base was membranous). Shells of *Au. modestus* and *T. rubescens* were composed of four parietal plates and lacked a mineralized base. At the meso-scale, shell plates varied in the presence of canals within the shell plates. Longitudinal canals within the parietal plates and radial canals within the base plate were observed in all *Amphibalanus* barnacles. Canals were also present in the parietal plates of *S. balanoides* and *T. rubescens*. Shell plates were solid (i.e., lacked canals) in *Au. modestus* and *C. stellatus*.

For lab-reared barnacles (grown for the same duration and under the same environmental conditions), species identity had a strong effect on plate thickness, with thickness varying among species in both the parallel and perpendicular orientations (Table 1 and Figure 3). Parietal plates were about twice as thick in *Am. amphitrite* as compared to *Au. modestus*, with *Am. improvisus* intermediate to these species. Patterns of thickness with respect to orientation (parallel vs. perpendicular) were variable among species, likely reflecting the specific plane at which individual barnacles were polished and the angle of the parietal plates relative to the base. In species with a mineralized base plate (*Am. amphitrite* and *Am. improvisus*), parietal plates were on average 5.3 times thicker than the base plate within the same individual (Figure 3; Table S1).

At the micron-scale, SEM imaging (conducted in a central portion of the plates away from plate boundaries) revealed that shell plates from all species were composed of irregular, micron-scale crystallites (parietal plates: Figure 2B; base plate; Figure S1). A heterogeneous mix of crystallite dimensions and morphologies was observed in all plates examined, with the maximum width of crystals varying by an order of magnitude within the same 25 × 19 µm imaged region. For example, in *S. balanoides* measured crystal width ranged from ~500 nm to 5 µm; similar patterns were observed for other species and for samples oriented in both the parallel and perpendicular orientation (Table S2).

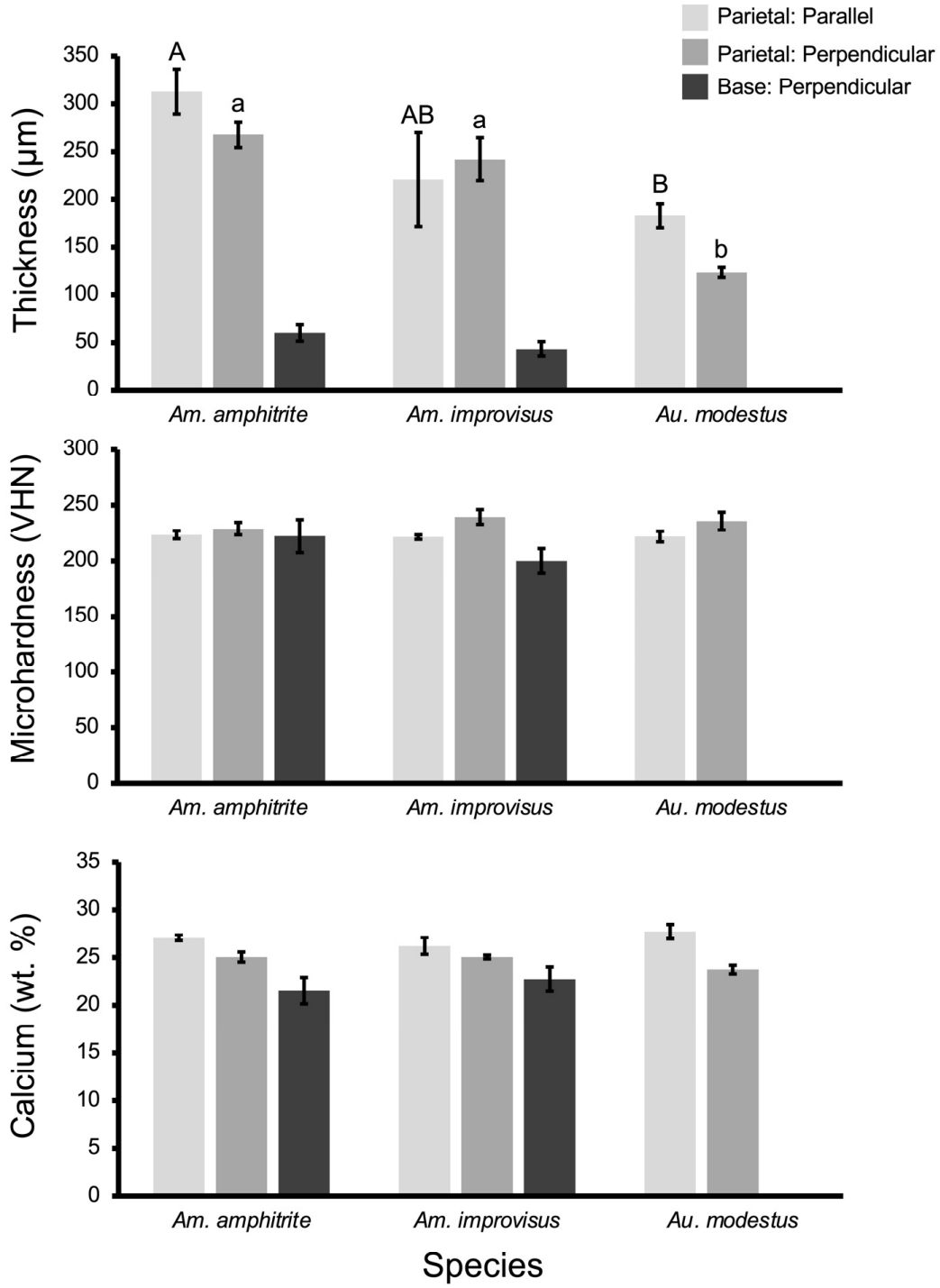

Figure 3. Shell plate thickness, microhardness, and calcium content for lab-reared barnacles (means ± S.E.). Testing was conducted with shells oriented parallel to, or perpendicular to, the base. Note that *Au. modestus* lacks a mineralized base plate. For thickness, letters represent results of pairwise comparisons within the same orientation; species marked with different letters have means that are statistically different from one another, whereas those that share a letter do not differ (Tukey HSD: $p < 0.05$). Uppercase letters denote pair-wise differences between species when tested in the parallel orientation, and lowercase letters denote pair-wise differences between species when tested in the perpendicular orientation. Microhardness and calcium content did not differ among species (One-way ANOVA: $p > 0.05$). n = 4–5 per species, per orientation for thickness and microhardness; n = 3 per species, per orientation for calcium content.

Table 1. One-way ANOVA assessing the effect of species identity on plate thickness, microhardness, and calcium content in lab-reared species. df = degrees of freedom; F and *p* are outcomes of the statistical tests, where F refers to the F-statistic and *p* is probability of the null hypothesis (no difference). A *p*-value less than 0.05 is considered statistically significant. Effect sizes are reported as η^2. For reference, η^2 above 0.14 is considered a large effect and above 0.06 is a medium effect [31].

Variable	df	F	*p*	η^2
Plate thickness				
Parallel	13	5.635	0.021	0.506
Perpendicular	13	47.65	0.000	0.897
Microhardness				
Parallel	14	0.093	0.911	0.015
Perpendicular	13	0.588	0.572	0.097
Calcium content				
Parallel	8	1.189	0.367	0.284
Perpendicular	8	3.285	0.109	0.523

3.2. Mechanical Properties

Microhardness did not vary among lab-reared barnacle species in either the parallel or perpendicular orientation, with species identity explaining little of the variance among data (Table 1 and Figure 3). On average, microhardness tended to be slightly (~5%) higher when shells were tested in the perpendicular orientation, but patterns with respect to orientation were variable among individual barnacles. When comparing parietal plates to the base plate of the same barnacle, parietal plates of *Am. improvisus* were consistently harder than the base of the same individual (on average ~21% harder). Microhardness of the parietal vs. base plate in *Am. amphitrite* was variable among individuals, with parietal plate microhardness higher in some individuals but base plate microhardness higher in others.

3.3. Composition

Barnacle shells from all species were composed of calcite with no other polymorphs of calcium carbonate present, as determined by FTIR spectroscopy (Figure 4). Calcite is characterized by a sharp ν_4 peak at 713 cm^{-1} and a ν_2 peak at 874 cm^{-1} [32], both of which are prominent in all shells assessed. Shells were composed primarily of O, C, and Ca (~98 wt% total among all species) with the remaining elemental content as Mg, Sr, S, P, Cl, Na, Si and Al (Table S1). Si and Al are likely residual from the polishing process. Calcium content in the shell did not differ among species when tested in either the parallel or perpendicular orientation (Table 1 and Figure 3). Parietal plate calcium content tended to be slightly (~9.8%) higher than when tested in the perpendicular orientation as compared to the parallel orientation. When tested within the same individual barnacle, calcium content was consistently higher in the parietal plate than the base plate (on average ~16.5% higher in the parietal plates).

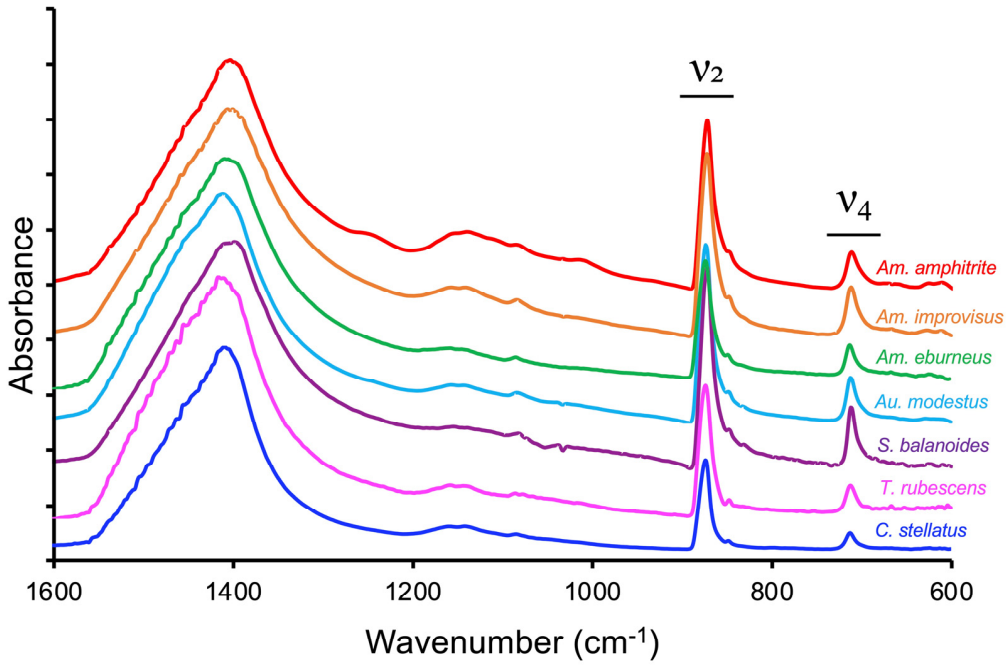

Figure 4. Representative FTIR spectra of powdered shell samples from seven species of barnacles. In all species tested, spectra are consistent with calcite, characterized by sharp ν_2 and ν_4 peaks at 874 cm^{-1} and 713 cm^{-1}, respectively.

4. Discussion

Acorn barnacles are completely reliant on a robust shell for defense against predators and protection from environmental stressors. Size and macro-scale shell structure varies markedly among Balanomorpha [8,11,33], as does macro-scale shell strength [18,19,34,35]. We sought to provide insight on the basis for such differences by characterizing the structure, micromechanical properties, and elemental composition of the shells of seven species of balanomorph barnacles from five genera. Three of these species were lab-reared under identical conditions, precluding the impact of environment or growth duration on shell properties. Among the species assessed, shell properties varied at the macro- and meso-scales in terms of the number of shell plates, the presence of canals within the plates, mineralization of the base, and shell plate thickness. Despite such macro- and meso-scale variation, we observed little variation among species at the micron-scale. Microhardness did not vary among species, all shells were composed of irregular micron-scale calcite crystallites, and calcium content was consistent among species. These observations suggest an evolutionarily conserved pathway for mineralization in Balanomorpha. Differences in macro-scale shell strength among species arise from variation in shell thickness and the assembly of shell plates rather than variation at the micron-scale.

At the macro- (whole-shell) scale, balanomorph barnacles typically display a truncated cone morphology, formed by mineralized parietal plates, and a flat bottom that is adhered to a solid surface [1,8,10]. As evidenced by the seven balanomorph species assessed here, however, variation on this common theme arises at the meso- (individual plate) scale. Five of the seven species examined (those in the superfamilies Coronuloidea and Balanoidea) possessed longitudinal canals (tubes) within the parietal plates and, among *Amphibalanus* species, radial canals within the calcified base plate. In contrast, shell plates were solid among Chthamaloidea and Elminoidea [8]. Canals within shell plates are lined with ion-rich epithelia [36], which appear to be an extension of, and continuous with, the mantle parenchyma [22,37,38]. Canal tissue is likely to play a role in biomineralization, potentially providing ions, enzymes (e.g., carbonic anhydrase), and other components necessary for shell formation [36,38,39]. Other roles that have been proposed for canal tissue, based on histological and proteomic assessments, include osmoregulation, adhesion,

and female reproduction [36,38–40]. In addition, the presence of canals within a solid shell plate can be beneficial mechanically, increasing overall strength (particularly if the region surrounding canals is reinforced) and toughness by disrupting the spread of cracks (i.e., crack trapping) [11,17].

Stability of the basal plate or membrane in balanormoph barnacles is critical to their success in challenging environments, since it serves as the sole point of attachment to the substrate and mediates adhesion [39,41–43]. Among Balanomorpha, mineralization of the base varies among phylogenetic groups [8] and of the species assessed here, only those in the genus *Amphibalanus* possessed a mineralized base. In *Amphibalanus amphitrite*, the base plate-substrate interface is complex, especially at the growth edge, with spatially distinct layers of calcite with distinct grain sizes and a layer of cuticle between the mineralized base and the cement [41,44]. This complex structure, along with the architecture of the junction of the base and parietal plates, enhances adhesion strength (resistance to removal) via a crack-trapping mechanism, as described in detail by Hui et al. [45]. Incipient crack energy is essentially diverted from the adhesive-substrate interface to the mineralized plate, encouraging fractures at the shell periphery but preserving the majority of the adhesive-substrate interface.

Whereas macro- and meso-scale structure varied among phylogenetic groups, shell plates from all species we assessed were composed of highly irregular crystallites. Maximum width of crystallites was, on average, ~1.5 μm, but dimensions of neighboring crystallites varied dramatically (i.e., often by nearly ten-fold) and individual crystals did not appear to take on a preferred or defined morphology. Further, there were no discernable differences in crystallite morphology or dimensions when shell plates were imaged parallel to, versus perpendicular to, the base. These observations align with those described previously in the bulk of the shell plates (away from plate junctions or growth margins) of *Amphibalanus amphitrite* [20,23,30], *Austromegabalanus psittacus*, *Perforatus perforatus* [21,22,46,47], and *Semibalanus balanoides* [24]. It is worth noting that other microstructures have been identified—for example, fibrous, elongated grains oriented perpendicular to the contact surface within growth margins of alae (parietal plate junctions) [21,24]—but the bulk of the shell is composed of irregular (or at times, roughly rhombohedral) crystallites. Quantitatively determining crystallographic orientation of the shell plates was beyond the scope of this study, but previous analyses documented variation in the extent of crystal co-orientation among regions of the shell, which was supported qualitatively by our polarized light microscopy imaging [21,23]. At least for *Amphibalanus amphitrite* and *Austromegabalanus psittacus* (both within the superfamily Balanoidea), individual crystallites tend to cluster, with multiple crystallites taking on the same orientation, forming what Checa et al. [21] refers to as "crystallographically coherent regions" or "CCRs". Similar to the crystallites themselves, CCRs vary dramatically in morphology and dimensions [21,23]. Quantitative assessments of crystallographic orientation in Coronuloidea, Chthamaloidea, and Elminoidea are currently lacking.

The parietal plates of barnacles from all phylogenetic groups were composed of calcite with no other polymorphs of calcium carbonate identified. Construction of parietal plates from calcite appears to be universal among the balanomorph species assessed to date [8,33,48,49]. Early reports noted the presence of aragonite within the mineralized base plate of two warm-water *Tetraclita* species (Coronuloidea) and *Catophragmus imbricatus* (Chthamaloidea) [49], but more recent work on the base plate of *Amphibalanus amphitrite*, also a warm-water species, identified only calcite [41]. Checa et al. [46] suggest the presence of amorphous calcium carbonate (ACC) in parietal plates based on crystallite morphology and orientation, thermodynamics of crystal growth, and coupled X-ray diffraction (XRD) with thermogravimetric analysis (TGA)-differential scanning calorimetry (DSC). Hur et al. [43] identified metastable vaterite based on in vitro nucleation assays with a basally expressed, recombinant cement protein (MrCP-19) known to interact with calcite. Both studies hypothesize a role for these transient mineral phases in the shell-formation process. Although neither polymorph of calcium carbonate was identified here, if present,

their transient nature [50] and low abundance within the adult shell plate [46] would make detection challenging.

Balanomorph barnacles incorporate calcium and other ions from external seawater as they form their shell [51,52], likely mediated by cells of the mantle epithelium [36,53]. Elemental composition of the shell, and the proportion of trace elements in relation to calcium, have been shown to vary with growth conditions, including tidal height (and therefore, immersion time), temperature, salinity, and trace metal content of seawater [52,54–56]. Bourget [54] also reported a limited number of statistically significant pairwise differences in trace metal to calcium ratios between species when collected from the same field site (and presumably similar environmental conditions). These responses, however, were complex, and patterns differed when comparing the same species at different tidal heights. Among the lab-reared barnacles assessed here, calcium content did not differ among species, regardless of testing orientation, and the suite of elements identified was the same in all cases. Hence, when grown under the same conditions and for the same duration, calcium content in the shell is relatively consistent, at least for the species (and conditions) tested here. We were unable to track environmental conditions or growth duration for field-collected samples in this study. Paired field and lab studies where environmental conditions and growth duration are closely monitored and systematically adjusted would provide insight into the complex patterns of elemental uptake in balanomorph shells.

The microhardness of a biomineral is the product of a range of factors, including the material's mineral content (both the abundance and identity of ions), polymorph(s) of mineral present, crystal morphology, orientation, density, and assembly with organic components/matrix, organic inclusions within crystals, and composition and cross-linking of organic components [57–60]. Given the similarity in microstructure, calcium carbonate polymorph, and elemental composition observed here, it is not surprising that microhardness did not vary among the species tested. There are few comparative reports of balanomorph shell plate microhardness available, but similar to what was observed here, Murdock and Currey [19] reported no difference in microhardness (or microstructure) of shell plates between *Balanus balanus* and *Semibalanus balanoides*, despite *Balanus balanus* displaying about four-fold higher macro-scale shell strength.

When comparing shell plate properties among individuals of the same species, two general trends emerge. First, in species with a mineralized base plate, properties of the base differed from those of the parietal plates. Although micron-scale morphology was largely similar among the plates, calcium content was consistently lower, and magnesium content higher, in the base plate compared to the parietal plates of the same individual. In *Amphibalanus improvisus*, microhardness of the base plate was also lower than that of the parietal plates, consistent with previous mechanical assessments in *Amphibalanus reticulatus* [61]. These findings suggest that mineralization processes vary between the base and parietal plates. Such variation may be driven by differences in the type and abundance of organic matrix proteins in the base and parietal plates [39]. Second, parietal plates exhibited slight anisotropy at the micron-scale. Parietal plates cross-sectioned parallel to the base exhibited higher calcium content but slightly lower microhardness compared to those cross-sectioned perpendicular to the base. The factors driving this anisotropy are unclear, particularly since the morphology of calcite crystallites appeared similar in both directions. Given the dramatic differences in shell thickness and architecture at the meso- and macro-scales [17–19,48], the impact of this subtle anisotropy on whole-shell mechanics is likely to be minimal.

5. Conclusions

The mechanisms by which balanomorph barnacles construct their shells—including the extent of biological control vs. organization by crystal growth [21,46,47] and the identity, role, and source of proteins (including enzymes) and other macromolecules involved in shell formation [39,40,43,47,62]—are an active area of investigation. Similarities observed here among species in terms of the irregular morphology of bulk-shell crystallites, calcium

carbonate polymorph, elemental content, and micromechanical properties, suggest a highly conserved pathway for mineralization among Balanomorpha. Common micron-scale building blocks are then woven into very different meso- and macro-scale structures, resulting in variations in plate thickness, architecture, and morphology, and hence, differences in macro-scale mechanical properties. Future investigations on how each level of biological complexity is affected by alterations in environmental conditions (e.g., salinity, temperature, pH/ocean acidification) and physical and chemical properties of the substrate on which balanomorph larvae settle (including the presence of chemical additives, e.g., antifouling agents) would shed light on the pathways of biomineralization and may help to identify points within that pathway that may weaken shells for fouling mitigation efforts.

Supplementary Materials: The following supporting information can be downloaded at: https://www.mdpi.com/article/10.3390/d16080482/s1, Figure S1: SEM imaging of barnacle base plates; Table S1: Quantitative dataset; Table S2: Maximum calcite crystal width measurements.

Author Contributions: Conceptualization, G.H.D. and R.A.M.; Methodology, G.H.D., R.A.M. and N.A.; Validation, G.H.D. and R.A.M.; Formal Analysis, J.S. and G.H.D.; Investigation, J.S., C.T., Y.K. and C.J.H.; Resources, G.H.D., R.A.M. and N.A.; Data Curation, J.S. and G.H.D.; Writing—Original Draft Preparation, J.S. and G.H.D.; Writing—Review and Editing, G.H.D., R.A.M. and N.A.; Visualization, J.S. and G.H.D.; Supervision, G.H.D. and R.A.M.; Project Administration, G.H.D., R.A.M. and N.A.; Funding Acquisition, G.H.D. and R.A.M. All authors have read and agreed to the published version of the manuscript.

Funding: Financial support was provided by an NSF Divisions of Material Research grant to G.H.D. (award #1905466) and R.A.M. (award #1905619).

Institutional Review Board Statement: Not applicable.

Data Availability Statement: Data are available within the Supplementary Materials.

Acknowledgments: The authors gratefully acknowledge Manuel Figueroa (The College of New Jersey) for providing substrates for barnacle settlement and Roland Hagan and Miranda Rosen (Rutgers University Marine Field Station) for assistance with barnacle collection and field assays. We thank Isra Ahmad and Sameer Kamal for assistance with data collection and Keith Pecor for consultation on statistical analyses.

Conflicts of Interest: The authors declare no conflicts of interest.

References

1. Pérez-Losada, M.; Høeg, J.T.; Simon-Blecher, N.; Achituv, Y.; Jones, D.; Crandall, K.A. Molecular phylogeny, systematics and morphological evolution of the acorn barnacles (Thoracica: Sessilia: Balanomorpha). *Mol. Phylogen. Evol.* **2014**, *81*, 147–158. [CrossRef] [PubMed]
2. Barnes, M. The use of intertidal barnacle shells. In *Oceanography and Marine Biology: An Annual Review*; Gibson, R.N., Barnes, M., Eds.; Taylor & Francis: London, UK, 2000; Volume 38, pp. 157–187.
3. Jernakoff, P. Factors affecting the recruitment of algae in a midshore region dominated by barnacles. *J. Exp. Mar. Biol. Ecol.* **1983**, *67*, 17–31. [CrossRef]
4. Reimer, A. Description of a *Tetraclita stalactifera panamensis* community on a rocky intertidal Pacific shore of Panama. *Mar. Biol.* **1976**, *35*, 225–238. [CrossRef]
5. Sarkar, P.K.; Pawar, S.S.; Rath, S.K.; Kandasubramanian, B. Anti-barnacle biofouling coatings for the protection of marine vessels: Synthesis and progress. *Environ. Sci. Pollut. Res.* **2022**, *29*, 26078–26112. [CrossRef] [PubMed]
6. Thomason, J.C.; Hills, J.M.; Clare, A.S.; Neville, A.; Richardson, M. Hydrodynamic consequences of barnacle colonization. *Hydrobiologia* **1998**, *376*, 191–201. [CrossRef]
7. Lively, C.M. Competition, comparative life histories, and maintenance of shell dimorphism in a barnacle. *Ecology* **1986**, *67*, 858–864. [CrossRef]
8. Chan, B.K.; Dreyer, N.; Gale, A.S.; Glenner, H.; Ewers-Saucedo, C.; Pérez-Losada, M.; Kolbasov, G.A.; Crandall, K.A.; Høeg, J.T. The evolutionary diversity of barnacles, with an updated classification of fossil and living forms. *Zool. J. Linn. Soc.* **2021**, *193*, 789–846. [CrossRef]
9. Seoane Miraz, D. Genetic Analyses in the Gooseneck Barnacles (genus *Pollicipes*). Ph.D. Theses, Universidad de Coruña, Coruña, Spain, 2015.
10. Anderson, D.T. *Barnacles: Structure, Function, Development and Evolution*; Chapman & Hall: London, UK, 1994; p. 357.
11. Crisp, D.J.; Bourget, E. Growth in barnacles. *Adv. Mar. Biol.* **1985**, *22*, 199–244. [CrossRef]

12. Matsumura, K.; Qian, P.-Y. Larval vision contributes to gregarious settlement in barnacles: Adult red fluorescence as a possible visual signal. *J. Exp. Biol.* **2014**, *217*, 743–750. [CrossRef]
13. Darwin, C.R. *A Monograph on the Sub-Class Cirripedia: The Balanidć (or Sessile Cirrepedes) the Verrucidć, etc., etc., etc.*; Ray Society: London, UK, 1854; Volume 2, p. 684.
14. Pitombo, F.B. Comparative morphology of the Balanidae (Cirripedia): A primer to a phylogenetic analysis. In *Crustaceans and the Biodiversity Crisis*; Schram, F., von Vaupel Klein, C., Eds.; Brill: Amsterdam, The Netherlands, 1999; pp. 151–171.
15. Pitombo, F.B. Phylogenetic analysis of the Balanidae (Cirripedia, Balanomorpha). *Zool. Scr.* **2004**, *33*, 261–276. [CrossRef]
16. Trenn, T.J. Charles Darwin, fossil cirripedes, and Robert Fitch: Presenting sixteen hitherto unpublished Darwin letters of 1849 to 1851. *Proc. Am. Philos. Soc.* **1974**, *118*, 471–491.
17. Astachov, L.; Nevo, Z.; Brosh, T.; Vago, R. The structural, compositional and mechanical features of the calcite shell of the barnacle *Tetraclita rufotincta*. *J. Struct. Biol.* **2011**, *175*, 311–318. [CrossRef] [PubMed]
18. Barnes, H.; Read, R.; Topinka, J. The behaviour on impaction by solids of some common cirripedes and relation to their normal habitat. *J. Exp. Mar. Biol. Ecol.* **1970**, *5*, 70–87. [CrossRef]
19. Murdock, G.R.; Currey, J.D. Strength and design of shells of the two ecologically distinct barnacles, *Balanus balanus* and *Semibalanus* (*Balanus*) *balanoides* (Cirripedia). *Biol. Bull.* **1978**, *155*, 169–192. [CrossRef]
20. Khalifa, G.M.; Weiner, S.; Addadi, L. Mineral and matrix components of the operculum and shell of the barnacle *Balanus amphitrite*: Calcite crystal growth in a hydrogel. *Cryst. Growth Des.* **2011**, *11*, 5122–5130. [CrossRef]
21. Checa, A.G.; González-Segura, A.; Rodríguez-Navarro, A.B.; Lagos, N.A. Microstructure and crystallography of the wall plates of the giant barnacle *Austromegabalanus psittacus*: A material organized by crystal growth. *J. R. Soc. Interface* **2020**, *17*, 20190743. [CrossRef] [PubMed]
22. Checa, A.G.; Salas, C.; Rodríguez-Navarro, A.B.; Grenier, C.; Lagos, N.A. Articulation and growth of skeletal elements in balanid barnacles (Balanidae, Balanomorpha, Cirripedia). *R. Soc. Open Sci.* **2019**, *6*, 190458. [CrossRef]
23. Lewis, A.C.; Burden, D.K.; Wahl, K.J.; Everett, R.K. Electron backscatter diffraction (EBSD) study of the structure and crystallography of the barnacle *Balanus amphitrite*. *JOM* **2014**, *66*, 143–148. [CrossRef]
24. Mitchell, R.; Coleman, M.; Davies, P.; North, L.; Pope, E.; Pleydell-Pearce, C.; Harris, W.; Johnston, R. Macro-to-nanoscale investigation of wall-plate joints in the acorn barnacle *Semibalanus balanoides*: Correlative imaging, biological form and function, and bioinspiration. *J. R. Soc. Interface* **2019**, *16*, 20190218. [CrossRef]
25. Meyers, M.A.; Chen, P.-Y.; Lopez, M.I.; Seki, Y.; Lin, A.Y. Biological materials: A materials science approach. *J. Mech. Behav. Biomed. Mater.* **2011**, *4*, 626–657. [CrossRef]
26. Meyers, M.A.; McKittrick, J.; Chen, P.-Y. Structural biological materials: Critical mechanics-materials connections. *Science* **2013**, *339*, 773–779. [CrossRef] [PubMed]
27. Rittschof, D.; Branscomb, E.; Costlow, J. Settlement and behavior in relation to flow and surface in larval barnacles, *Balanus amphitrite* Darwin. *J. Exp. Mar. Biol. Ecol.* **1984**, *82*, 131–146. [CrossRef]
28. Rittschof, D.; Clare, A.; Gerhart, D.; Mary, S.A.; Bonaventura, J. Barnacle in vitro assays for biologically active substances: Toxicity and settlement inhibition assays using mass cultured *Balanus amphitrite amphitrite* Darwin. *Biofouling* **1992**, *6*, 115–122. [CrossRef]
29. Figueroa, M.A.; Schablik, J.D.; Mastroberte, M.; Singh, L.; Dickinson, G.H. The effect of hydrophobic alkyl silane self-assembled monolayers on adult barnacle adhesion. *Mar. Technol. Soc. J.* **2017**, *51*, 39–48. [CrossRef]
30. Nardone, J.A.; Patel, S.; Siegel, K.R.; Tedesco, D.; McNicholl, C.G.; O'Malley, J.; Herrick, J.; Metzler, R.A.; Orihuela, B.; Rittschof, D.; et al. Assessing the impacts of ocean acidification on adhesion and shell formation in the barnacle *Amphibalanus amphitrite*. *Front. Mar. Sci.* **2018**, *5*, 369. [CrossRef]
31. Lakens, D. Calculating and reporting effect sizes to facilitate cumulative science: A practical primer for t-tests and ANOVAs. *Front. Psychol.* **2013**, *4*, 863. [CrossRef]
32. Chakrabarty, D.; Mahapatra, S. Aragonite crystals with unconventional morphologies. *J. Mater. Chem.* **1999**, *9*, 2953–2957. [CrossRef]
33. Bourget, E. Barnacle shells: Composition, structure and growth. In *Barnacle Biology*; Crustacean Issues; Southward, A.J., Schram, F.R., Eds.; A.A. Balkema: Rotterdam, The Netherlands, 1987; Volume 5, pp. 267–285.
34. Gubbay, S. Compressive and adhesive strengths of a variety of British barnacles. *J. Mar. Biol. Assoc. U. K.* **1983**, *63*, 541–555. [CrossRef]
35. Karande, A.; Udhayakumar, M. Shell structure and shell strength in Cirripedes. *Proc. Anim. Sci.* **1989**, *98*, 223–231. [CrossRef]
36. Gohad, N.V.; Dickinson, G.H.; Orihuela, B.; Rittschof, D.; Mount, A.S. Visualization of putative ion-transporting epithelia in *Amphibalanus amphitrite* using correlative microscopy: Potential function in osmoregulation and biomineralization. *J. Exp. Mar. Biol. Ecol.* **2009**, *380*, 88–98. [CrossRef]
37. Costlow, J.D. Shell development in *Balanus improvisus* Darwin. *J. Morphol.* **1956**, *99*, 359–415. [CrossRef]
38. Wang, C.; Schultzhaus, J.N.; Taitt, C.R.; Leary, D.H.; Shriver-Lake, L.C.; Snellings, D.; Sturiale, S.; North, S.H.; Orihuela, B.; Rittschof, D. Characterization of longitudinal canal tissue in the acorn barnacle *Amphibalanus amphitrite*. *PLoS ONE* **2018**, *13*, e0208352. [CrossRef] [PubMed]
39. Schultzhaus, J.; Hervey, J.; Fears, K.; Spillmann, C. Proteomic comparison of the organic matrices from parietal and base plates of the acorn barnacle *Amphibalanus amphitrite*. *Open Biol.* **2024**, *14*, 230246. [CrossRef] [PubMed]

40. Schultzhaus, J.N.; Wang, C.; Patel, S.; Smerchansky, M.; Phillips, D.; Taitt, C.R.; Leary, D.H.; Hervey, J.; Dickinson, G.H.; So, C.R. Distribution of select cement proteins in the acorn barnacle *Amphibalanus amphitrite*. *Front. Mar. Sci.* **2020**, *7*, 586281. [CrossRef]
41. De Gregorio, B.T.; Stroud, R.M.; Burden, D.K.; Fears, K.P.; Everett, R.K.; Wahl, K.J. Shell structure and growth in the base plate of the barnacle *Amphibalanus amphitrite*. *ACS Biomater. Sci. Eng.* **2015**, *1*, 1085–1095. [CrossRef] [PubMed]
42. Dickinson, G.H.; Vega, I.E.; Wahl, K.J.; Orihuela, B.; Beyley, V.; Rodriguez, E.N.; Everett, R.K.; Bonaventura, J.; Rittschof, D. Barnacle cement: A polymerization model based on evolutionary concepts. *J. Exp. Biol.* **2009**, *212*, 3499–3510. [CrossRef] [PubMed]
43. Hur, S.; Méthivier, C.; Wilson, A.; Salmain, M.; Boujday, S.; Miserez, A. Biomineralization in barnacle base plate in association with adhesive cement protein. *ACS Appl. Bio Mater.* **2023**, *6*, 3423–3432. [CrossRef] [PubMed]
44. Burden, D.K.; Spillmann, C.M.; Everett, R.K.; Barlow, D.E.; Orihuela, B.; Deschamps, J.R.; Fears, K.P.; Rittschof, D.; Wahl, K.J. Growth and development of the barnacle *Amphibalanus amphitrite*: Time and spatially resolved structure and chemistry of the base plate. *Biofouling* **2014**, *30*, 799–812. [CrossRef] [PubMed]
45. Hui, C.-Y.; Long, R.; Wahl, K.J.; Everett, R.K. Barnacles resist removal by crack trapping. *J. R. Soc. Interface* **2011**, *8*, 868–879. [CrossRef]
46. Checa, A.G.; Macías-Sánchez, E.; Rodríguez-Navarro, A.B.; Sánchez-Navas, A.; Lagos, N.A. Origin of the biphase nature and surface roughness of biogenic calcite secreted by the giant barnacle *Austromegabalanus psittacus*. *Sci. Rep.* **2020**, *10*, 16784. [CrossRef]
47. Rodríguez-Navarro, A.B.; Grenier, C.; Checa, A.G.; Jiménez-López, C.; Sánchez-Sánchez, P.; Bertone, D.; Lagos, N.A. Role of the organic matter in the structural organization of giant barnacle *Austromegabalanus psittacus* shell from the micro-to nanoscale. *Cryst. Growth Des.* **2021**, *21*, 357–365. [CrossRef]
48. Bourget, E. Shell structure in sessile barnacles. *Nat. Can.* **1977**, *104*, 281–323.
49. Lowenstam, H.A. Coexisting calcites and aragonites from skeletal carbonates of marine organisms and their strontium and magnesium contents. In *Recent Researches in the Fields of Hydrosphere, Atmosphere and Nuclear Chemistry*; Miyake, Y., Koyama, T., Eds.; Maruzen Co., Ltd.: Tokyo, Japan, 1964; pp. 373–404.
50. Khouzani, M.F.; Chevrier, D.M.; Güttlein, P.; Hauser, K.; Zhang, P.; Hedin, N.; Gebauer, D. Disordered amorphous calcium carbonate from direct precipitation. *CrystEngComm* **2015**, *17*, 4842–4849. [CrossRef]
51. Bourget, E.; Crisp, D.J. Factors affecting deposition of shell in *Balanus balanoides* (L). *J. Mar. Biol. Assoc. U. K.* **1975**, *55*, 231–249. [CrossRef]
52. Hockett, D.; Ingram, P.; LeFurgey, A. Strontium and manganese uptake in the barnacle shell: Electron probe microanalysis imaging to attain fine temporal resolution of biomineralization activity. *Mar. Environ. Res.* **1997**, *43*, 131–143. [CrossRef]
53. Nousek, N.A. Shell formation and calcium transport in the barnacle *Chthamalus fragilis*. *Tissue Cell* **1984**, *16*, 433–442. [CrossRef] [PubMed]
54. Bourget, E. Environmental and structural control of trace elements in barnacle shells. *Mar. Biol.* **1974**, *28*, 27–36. [CrossRef]
55. Findlay, H.S.; Kendall, M.A.; Spicer, J.I.; Widdicombe, S. Post-larval development of two intertidal barnacles at elevated CO_2 and temperature. *Mar. Biol.* **2010**, *157*, 725–735. [CrossRef]
56. Piwoni-Piórewicz, A.S.; Strekopytov, S.; Humphreys-Williams, E.; Kukliński, P. Environmental variables affect the elemental composition of calcitic skeletons: A case study of barnacle *Amphibalanus improvisus* and bryozoan *Einhornia crustulenta* from the brackish Baltic Sea (Preprint). *SSRN*, 4616289. [CrossRef]
57. Cho, K.R.; Kim, Y.-Y.; Yang, P.; Cai, W.; Pan, H.; Kulak, A.N.; Lau, J.L.; Kulshreshtha, P.; Armes, S.P.; Meldrum, F.C. Direct observation of mineral–organic composite formation reveals occlusion mechanism. *Nat. Commun.* **2016**, *7*, 10187. [CrossRef]
58. Kim, Y.-Y.; Carloni, J.D.; Demarchi, B.; Sparks, D.; Reid, D.G.; Kunitake, M.E.; Tang, C.C.; Duer, M.J.; Freeman, C.L.; Pokroy, B. Tuning hardness in calcite by incorporation of amino acids. *Nat. Mater.* **2016**, *15*, 903. [CrossRef]
59. Kunitake, M.E.; Baker, S.P.; Estroff, L.A. The effect of magnesium substitution on the hardness of synthetic and biogenic calcite. *MRS Commun.* **2012**, *2*, 113–116. [CrossRef]
60. Meyers, M.A.; Chen, P.-Y. *Biological Materials Science: Biological Materials, Bioinspired Materials, and Biomaterials*; Cambridge University Press: Cambridge, MA, USA, 2014.
61. Raman, S.; Kumar, R. Construction and nanomechanical properties of the exoskeleton of the barnacle, *Amphibalanus reticulatus*. *J. Struct. Biol.* **2011**, *176*, 360–369. [CrossRef] [PubMed]
62. Han, Z.; Wang, Z.; Rittschof, D.; Huang, Z.; Chen, L.; Hao, H.; Yao, S.; Su, P.; Huang, M.; Zhang, Y.-Y. New genes helped acorn barnacles adapt to a sessile lifestyle. *Nat. Genet.* **2024**, *56*, 970–981. [CrossRef] [PubMed]